PARTICLE PRODUCTION RATIOS AT 21, 31, 45 AND 53 GeV IN THE CENTRE OF MASS

M. G. ALBROW, D. P. BARBER, A. BOGAERTS, B. BOŠNJAKOVIĆ, J. R. BROOKS, A. B. CLEGG, F. C. ERNÉ, C. N. P. GEE, A. D. KANARIS, A. LACOURT, D. H. LOCKE, P. G. MURPHY, A. RUDGE, J. C. SENS and F. Van der VEEN
CERN, Geneva, Switzerland,
Foundation for Fundamental Research on Matter F.O M , Utrecht, The Netherlands,
University of Lancaster U K ,
University of Manchester, U.K.

Received 7 April 1972

Particle production ratios have been measured for $\pi^{\pm}$, $K^{\pm}$, p and $\bar{p}$ at the CERN ISR.

A single arm spectrometer has been set up at the CERN proton-proton Intersecting Storage Rings in order to study the production of particles with momenta between 1 and 25 GeV/c and angles between 25 and 150 mrad with respect to the colliding beams. We report here on a first set of data obtained with the partly completed spectrometer on the ratios π^+/p, K^+/p, $\bar{p}/\pi^-$, K^-/π^- and π^+/π^-, taken at 21, 31, 45 and 53 GeV total energy $E_{c.m.}$ in the centre of mass (s = 440, 960, 2030 and 2820 GeV^2), at angles between 40 and 100 mrad and with momenta between 4 and 12 GeV/c. In terms of the variables $x = p_L/p_{max}$ and p_T, the data cover the intervals $0.15 < x < 0.5$ and $0.2 < p_T < 1.2$ GeV/c.

The experimental set-up is shown in fig. 1. The spectrometer is placed above one of the ISR beams downstream from intersection #2. Septum magnet S1 and Cerenkov counters C_1 and C_2 are placed on supports which allow for displacement and rotation in the vertical plane. They are aimed at the intersection in such a ways that particles produced in an interval $\theta \pm \Delta\theta$ and with momenta $p \pm \Delta p$ are transported to the centre of BM1 and on to BM3 and Cerenkov counter C_3. The acceptance of the Small Angle Spectrometer (S.A.S.) is ~10^{-4}sr and ±15% in momentum. Pairs of wire chambers with magnetostrictive read-out are placed before and behind BM1 and behind BM3. The chambers are triggered by a coincidence (ADFIJ) between scintillators placed as shown in fig.1. The scintillators I form a 4 element hodoscope, scintillators J a 2 element hodoscope.

Particles are identified with C_1, C_2 and C_3. C_1 and C_2 (ethylene filled, ~1.4 m long) are set to the same pressure and count π's and K's, C_3 (H_2 filled, 6 m long) counts π's only.

The Small Angle Monitor hodoscope (S.A.M.) placed around the beam pipe on the opposite side of the intersection to S.A.S. consists of five scintillators, one placed above and four below the pipe at 8 m from the intersection subtending angles from 20 mrad above to 100 mrad below the median plane.

For each event (as defined by the ADFIJ coincidence) the spark chamber coordinates, the re-

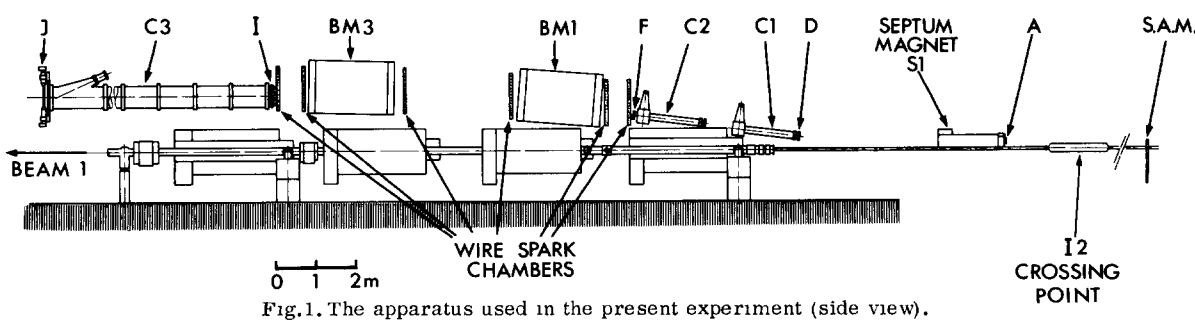

Fig.1. The apparatus used in the present experiment (side view).

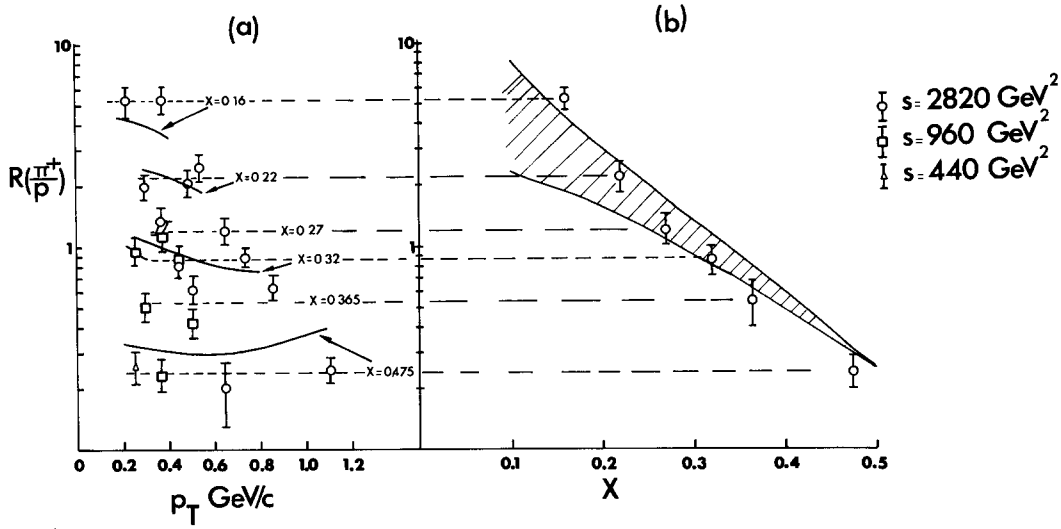

Fig.2. The π^+/p ratio versus p_T for various values of x (left) and versus x (averaged over the points at the left). The solid lines and the shaded area are the predictions of the thermodynamical model.

cords of all scintillators, the pulse heights of C_1, C_2, C_3 and the time of flight differences between the S.A.S. trigger and any of the S.A.M. counters are recorded on magnetic tape. The Cerenkov efficiencies are checked by applying cuts to the pulse height spectra whenever necessary.

The counting rate in S.A.S. ranges between 0.5 and 3 events /sec for $I_1 \times I_2 \sim 5\ A^2$. Between 2000 and 10 000 events were recorded at each setting of p and θ; the results reported here cover 25 such sets of events.

A considerable, and at times strongly varying, fraction of events in S.A.S. is due to beam-gas and beam-pipe collisions within the solid angle subtended by the spectrometer. This contamination disappears when events are selected in coincidence with a S.A.M. count in the correct time interval, i.e., events originating from the region where the two beams cross. This follows from data taken with only the background producing beam (i.e. the beam passing underneath S.A.S.) present in the ISR, resulting in a negligible number of S.A.S./S.A.M. coincidences. In addition the rate of S.A.S./S.A.M. coincidences drops to negligible values when the two beams are vertically separated from each other. The procedure of excluding background by requiring a S.A.S./S.A.M. coincidence is (at least at present) to be preferred over subtracting the background by means of data taken, at some other time, with one beam in the ISR only, not only because of the added measuring time required but mostly since small changes in the machine conditions occurring more or less randomly in time often cause a considerable change in background.

The limitation of the S.A.M. requirement is that it may distort the particle ratios since, say, a proton in S.A.S. is not necessarily accompanied by the same particle configuration in the opposite direction as a pion. This would certainly be the case near the upper end of the momentum spectrum, $x \approx 1$, where there may be a large contribution from protons scattered elastically or quasi-elastically. The present data refer to

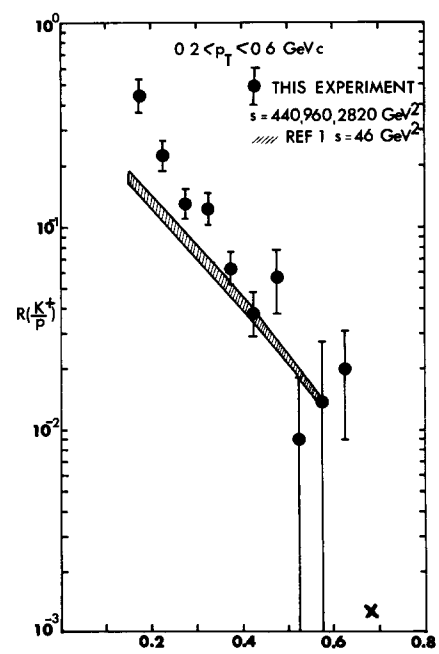

Fig.3. The K^+/p ratio versus x for $0.2<p_T<0.6$ GeV/c. Data at 24 GeV of ref. [1] are shown as a shaded area.

$x < 0.5$ and have been taken at angles which are too large for quasi-elastic contributions to be significant. Furthermore, at one ISR energy and one setting of S.A.S. the particle spectra in S A.S. obtained in coincidence with S.A.M. have been compared with those obtained from S.A.S. only, by subtracting "one-beam-only" data from "beam-beam + background" data; within the limited statistics there is agreement between the two sets of spectra. Finally, under "quiet" running conditions, typically 40% - 60% of the beam-beam events in S.A.S. are accompanied by a count in S.A.M. This fraction is large enough to give confidence that no serious bias is introduced. Nevertheless, the data are reported with the reservation that they may be distorted by the requirements on the opposite "jet".

The data are shown in figs. 2 to 5. The ratios are defined as

$$R(\pi^+/\mathrm{p}) = \left[\frac{\mathrm{d}^2\sigma}{\mathrm{d}x\mathrm{d}p_T^2}\right]_{\pi^+} \Big/ \left[\frac{\mathrm{d}^2\sigma}{\mathrm{d}x\mathrm{d}p_T^2}\right]_{\mathrm{p}} \quad .^*$$

The rates have been corrected for decay in the 30 m long spectrometer and for absorption of π, K, $\bar{\mathrm{p}}$ and p in the vacuum pipe walls and the scintillators in S.A.S. These corrections may introduce systematic errors which we believe to be less than 10%. The errors presented are statistical only.

(i) π^+/p ratio. Data were taken at $0.15 < x < 0.5$ and $0.2 < p_T < 1.1$ GeV/c at s = 440, 960 and 2820 GeV^2. Fig.2a shows $R(\pi^+/\mathrm{p})$ binned in x and p_T for these three values of s. It appears that the π^+/p ratio is essentially independent of s, within the typically 10% statistical errors. Furthermore the ratio is essentially constant in p_T, for $p_T >$ 0.2 GeV/c. Hence the production cross sections for π^+ and p have the same s and p_T dependence and this ratio appears to be a function of x only. Averaging over p_T we obtain the x-dependence shown in fig.2b.

The ratios have been compared with the data of Allaby et al. at 24 GeV incident energy on a stationary target. In the range of x covered by the present experiment the π^+/p ratios at 24 GeV and at ISR energies are in general agreement.

We have also compared the data with the thermodynamical model of Hagedorn and Ranft [2]. The solid lines in fig.2a show the results of this calculation at x = 0.16, 0.22, 0.32 and 0.475 for

* An alternative definition is $R = (E\mathrm{d}^2\sigma/\mathrm{d}x\mathrm{d}p_T^2)_\pi / (E\mathrm{d}^2\sigma/\mathrm{d}x\mathrm{d}p_T^2)_\mathrm{p}$, the difference is significant only near $x = 0$ at these energies, and is < 2.5% for our data.

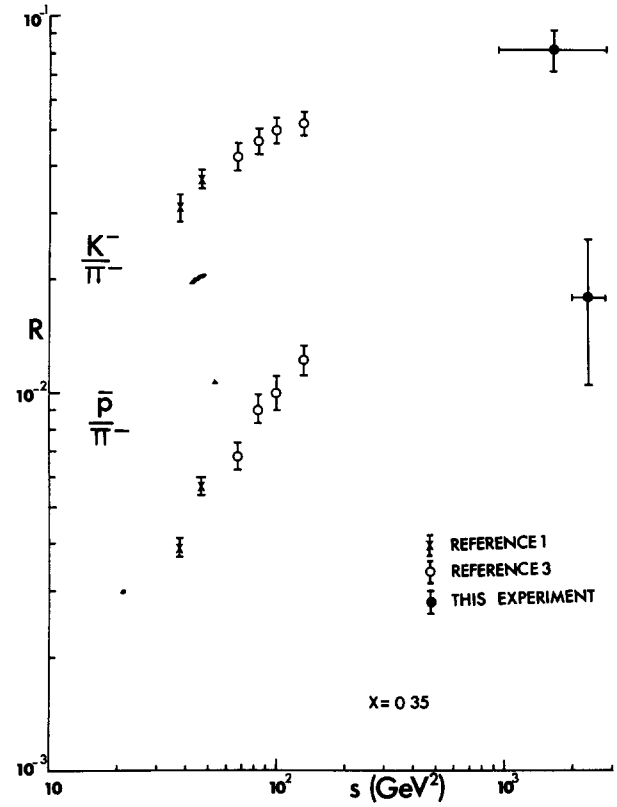

Fig.4. The K^-/π and $\bar{\mathrm{p}}/\pi^-$ ratios at $x \sim 0.35$ versus log s. The data are from refs. [1, 3] and this experiment.

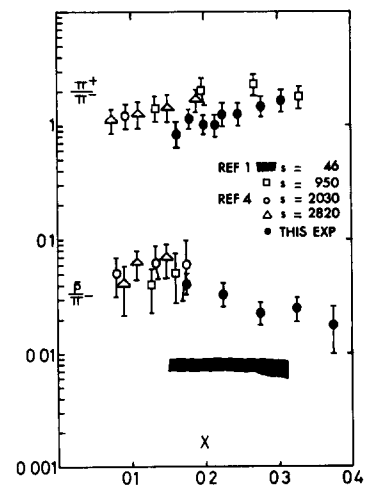

Fig.5. π^+/π^- ratio at s = 2820 GeV^2 and $0.4 < p_T < 0.9$ GeV/ $\bar{\mathrm{p}}/\pi^-$ ratio at s = 2030 and 2820 GeV^2 (averaged). The data of ref. [4] and thos of ref. [1] (at 24 GeV) are also shown.

$s = 960$ GeV^2. The ratio is essentially s-independent (to 10%) according to this model over the s-range covered. The general trend of the data seems to be well reproduced, but the data have a rather steeper s-dependence. The shaded area in fig.2b shows the range of the thermodynamical prediction for $960 < s < 2820$ GeV^2, $0 < p_T <$ GeV/c.

(ii) K^+/p ratio. The K^+/p ratio has been measured at $s = 440$, 960 and 2820 GeV^2. Comparing the ratios at 960 and 2820 GeV^2, where data were taken at the same intervals in x and p_T ($0.27 < x < 0.37$, $0.35 < p_T < 0.55$ GeV/c) we obtain:

$$R(K^+/p) = 0.09 \pm 0.025 \qquad s = 960 \text{ GeV}^2$$
$$= 0.11 \pm 0.02 \qquad s = 2820 \text{ GeV}^2$$

indicating that the ratio is independent of c.m. energy in this region of x and p_T. Combining all data with $0.2 < p_T \lesssim 0.6$ GeV/c and with $s = 440$, 960 and 2820 GeV^2 we obtain $R(K^+/p)$ as a function of x as shown in fig.3. Comparison with K^+/p ratios at 24 GeV of ref. [1] shows that, unlike the π^+/p ratio, the K^+/p ratio has grown at small x by a factor of ~ 2 between 24 GeV and ISR energies.

(iii) K^-/π^- ratio. Data have been obtained at $s = 960$, 2030 and 2820 GeV^2. Considering the s-dependence first, it is found that in the interval $0.3 < p_T < 0.5$ GeV/c, $0.1 < x < 0.4$ the K^-/π^- ratio remains constant to within a factor of two. Subdividing the x-range does not alter this conclusion. Binning the data into two intervals of x, one finds that the ratio is constant versus p_T, irrespective of s, while combining the data at all p_T the ratio appears to be constant versus x as well. We then average all data to get $R(K^-/\pi^-) = 0.082 \pm 0.010$ for $0.1 < x < 0.4$, $0.2 < p_T < 0.9$, $960 < s < 2820$ GeV^2.

For comparison the K^+/π^+ ratio averaged over the same range in x, p_T and s is $R(K^+/\pi^+) = 0.13 \pm 0.01$.

An average of the data of ref. [1] at 24 GeV over a similar range in x and p_T gives a K^-/π^- ratio of 0.037, indicating that a substantial increase occurs as the energy increases. In fig.4 we have compiled values of this ratio at $x \sim 0.35$ from Allaby et al. [1] and the results from Serpukhov of Binon et al. [3] (this data was taken with an Al target) plotted together with our point versus s. We conclude that if the π^- production cross-section have already reached a limiting value at accelerator energies [4], the K^- production cross-section continues to increase until at least $s = 1000$ GeV^2.

(iv) $\bar{p}/\pi^-$ ratio. Data have been obtained at $s = 2030$ and 2820 GeV^2. Averaging over these two s values and over the interval $0.2 < p_T < 0.9$ GeV/c one arrives at the x-dependence as shown in fig. 5. Also shown are the data of Bertin et al. [4], who find a ratio of 5% at $p_T = 0.4$ GeV/c and $0.07 < x < 0.2$, and the data at 24 GeV [1] ($s = 46$ GeV^2) which are a factor ~ 3 below those at ISR energies. We show in fig.4 these results together with those of Binon et al. [3] at $x \sim 0.35$, to illustrate the continual increase in the $\bar{p}$ production cross-section.

The thermodynamical model predicts correctly the shape of the x-distribution given by our data together with the data of ref. [4], and the magnitude of the increase between $s = 46$ and $s = 2000$ GeV^2.

(v) π^+/π^- ratio. The ratios quoted above are not affected by uncertainties in normalization, since at each x and p_T the two yields forming the ratio are measured simultaneously. For the ratio $R(\pi^+/\pi^-)$ the data have been normalized using a monitor, consisting of two telescopes of three scintillators each placed around the beam pipes. The π^+ and π^- data have been taken with the same stack circulating in the ISR. They were taken at $s = 2820$ GeV^2 and cover the range $0.15 < x < 0.3$ and $0.3 < p_T < 0.7$. The results (see fig.5) show that the π^+/π^- ratio increases away from ~ 1 as x increases. A similar result has been obtained by Bertin et al. from their data and that of ref. [5].

In conclusion the particle ratios show constancy over the s-range studied, but for K^+/p, $\bar{p}/\pi^-$, $\bar{K}/\pi^-$ in particular they have increased from the values measured at accelerator energies. The x-dependence of the ratios is in general accord with the predictions of the thermodynamical model. Towards small x, $x \sim 0.2$, the K^+/π^+ ratio (from $R(\pi^+/p)$ and $R(K^+/p)$) and the K^-/π^- ratio become similar, 9-12%, while the π^+/π^- ratio approaches 1. Furthermore reasonable extrapolations of the $\bar{p}/\pi^-$ and π^+/p ratios to $x = 0$ would give ~ 0.1 and ~ 10, implying $\bar{p}/p \sim 1$. This indicates that in the central region, $x \to 0$, $s \to \infty$, all particle and antiparticle yields may become equal.

We are grateful to Professors B. Gregory, W. Jentschke and Johnsen for their support in making this experiment possible. The assistance of the experimental support group, under the direction of F. Bonaudi, has been invaluable in setting up the apparatus. We thank the ISR vacuum group and the power supply group for their contributions in creating optimum conditions for the running of the experiment. We wish to thank M. Arbet and M. Keller for their skillful help, and J. Ranft for allowing us to use his computer program. This

work was supported in part by the Stichting voor Fundamenteel Onderzoekder Materie (F.O.M.) which is supported by the Nederlandse Organisatie voor Zuiver Wetenschappelijk Onderzoek (Z.W.O.) and in part by the Science Research Council through Daresbury Nuclear Physics Laboratory.

References

[1] J. V. Allaby, A. N. Diddens, R. W. Dobinson, A. Klovning, J. Litt, L. S. Rochester, K. Schlüpmann, A. M. Wetherell, U. Amaldi, R. Biancastelli, C. Bosio and G. Matthiae, to be published.
[2] R. Hagedorn and J. Ranft, CERN report TH-1440 (1972).
[3] F. Binon et al., Phys. Letters 30B (1969) 506.
[4] A. Bertin et al., Phys. Letters 38B (1972) 260.
[5] L. G. Ratner, R. J. Ellis, G. Vannini, B. A. Babcock, A. D. Krisch and J. B. Roberts, Phys. Rev. Letters 27 (1971) 68.

* * * * *